

See discussions, stats, and author profiles for this publication at: <https://www.researchgate.net/publication/375927335>

Voronoi Entropy as a Ligand Molecular Descriptor of Protein–Ligand Interactions

Article in ACS Omega · November 2023

DOI: 10.1021/acsomega.3c07328

CITATIONS
0

READS
57

4 authors:



Sergey Shityakov
University of Wuerzburg
165 PUBLICATIONS 1,841 CITATIONS

[SEE PROFILE](#)



Ekaterina Skorb
Max Planck Institute of Colloids and Interfaces
180 PUBLICATIONS 3,536 CITATIONS

[SEE PROFILE](#)



Aleksandr Sergeevich Aglikov
ITMO University
16 PUBLICATIONS 16 CITATIONS

[SEE PROFILE](#)



Michael Nosonovsky
University of Wisconsin - Milwaukee
205 PUBLICATIONS 9,455 CITATIONS

[SEE PROFILE](#)

Voronoi Entropy as a Ligand Molecular Descriptor of Protein–Ligand Interactions

Sergey Shityakov,* Aleksandr S. Aglikov, Ekaterina V. Skorb, and Michael Nosonovsky*



Cite This: <https://doi.org/10.1021/acsomega.3c07328>



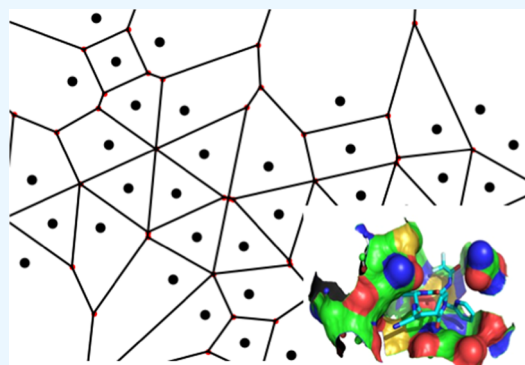
Read Online

ACCESS |

Metrics & More

Article Recommendations

ABSTRACT: We investigate the correlation between the Voronoi entropy (VE) of ligand molecules and their affinity to receptors to test the hypothesis that less ordered ligands have higher mobility of molecular groups and therefore a higher probability of attaching to receptors. VE of 1144 ligands is calculated using SMILES-based 2D graphs representing the molecular structure. The affinity of the ligands with the SARS-CoV-2 main protease is obtained from the BindingDB Database as half-maximal inhibitory concentration (IC_{50}) data. The VE distribution is close to the Gaussian, $0.4 \leq S_v \leq 1.66$, and a strong correlation with IC_{50} is found, $IC_{50} = -275 S_v + 613$ nM, indicating the correlation between ligand complexity and affinity. On the contrary, the Shannon entropy (SE) descriptor failed to provide enough evidence to reject the null hypothesis (p -value > 0.05), indicating that the spatial arrangement of atoms is crucial for molecular mobility and binding.



1. INTRODUCTION

Receptor–ligand interactions (RLIs) play an important role in many biological processes such as drug metabolism and neurotransmission. The RLI is often viewed as a “key–lock” interaction with a relatively large protein receptor molecule being a “lock” and a relatively small organic ligand molecule being a “key.” It is very difficult to predict whether two particular molecules would have a biospecific interaction between them, with one serving as a “key” corresponding to another’s “lock.” Various qualitative and quantitative measures and parameters have been suggested to estimate whether such an interaction is likely to happen between two particular molecules. Thus, Ballester and co-workers investigated machine learning methods to predict protein–ligand binding affinity with different scoring functions and emphasized poor predictivity for those complexes that do not conform to the modeling assumptions.¹ Persistent spectral-based machine learning was applied for binding affinity prediction.² Topology-based methods, such as persistent homology, have been used as well.³

One approach relies on the concepts of orderliness and symmetry. It is argued that less symmetric and less ordered ligands have a higher mobility than their more symmetric and ordered counterparts. This is because molecules lacking symmetry and orderliness have larger configurational space and, consequently, higher chances of forming a strong bond. Therefore, more complex ligands are more likely to possess better affinity to the protein molecules due to their conformational “compatibility” with the receptor binding sites. There are different measures of symmetry and orderliness

used in chemistry, including the continuous symmetry (CS) measure and Voronoi entropy (VE), which is also related to Shannon entropy (SE) information contained in a structure.^{4–8} CS does not necessarily correlate with VE and SE and can even anticorrelate.^{6,7} The concept of “near-symmetry” has been suggested as an extension of the CS.⁹ While SE relies on the relative frequencies of symbols in the string of symbols describing a system, VE uses instead the relative frequencies of polygons with different numbers of edges (triangles, tetragons, pentagons, hexagons, etc.) corresponding to data points in the 2D plane. In other words, polygons serve as “alphabetic symbols” for VE, similar to text characters for SE.

Ligands are small drug-like molecules in comparison with proteins, typically of less than 100 atoms. Unlike proteins, they usually do not possess a complex 3D secondary and tertiary structure and often can be viewed schematically as 2D planar molecules. This makes VE, which is a measure of the orderliness of 2D point sets, an appropriate measure to characterize the ligand’s orderliness.

VE is calculated for a set of points on a 2D plane from the Voronoi diagrams, where the plane is divided into domains or

Received: September 22, 2023

Revised: November 14, 2023

Accepted: November 16, 2023

cells based on the nearest point (Figure 1). The VE quantifies the orderliness of the sets of points and it is defined as

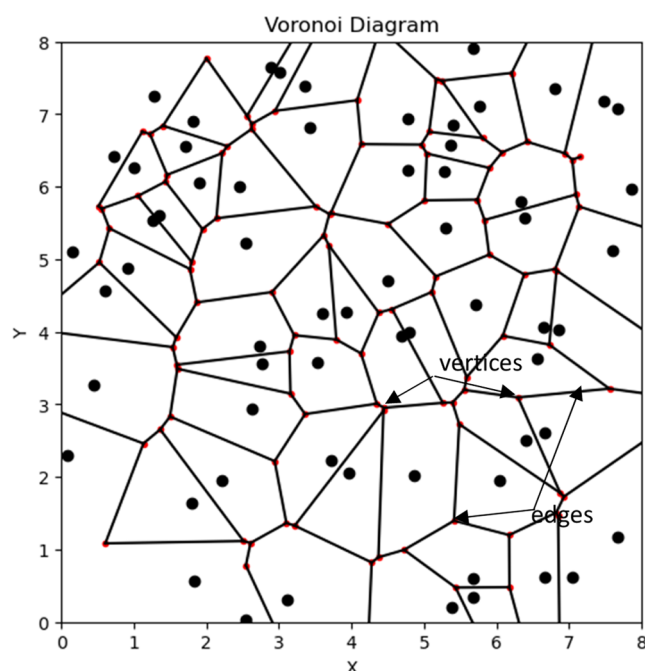


Figure 1. Example of a Voronoi diagram for a set of random points ($S_v = 1.54$).

$$S_v = - \sum_n P_n \ln P_n$$

where P_n is the fraction of n -sided polygons in a Voronoi diagram. The summation is performed from $n = 3$ to the largest number of polygon edges in the diagram. The VE is zero for an ordered system consisting of a single type of polygons (thus, for squares, $P_3 = 0$ and $P_4 = 1$ so that $\ln P_4 = 0$ and $S_v = 0$). For a random set of points, it has been found experimentally that the value of VE is $S_v = 1.71$, so the value of VE in the range $0 \leq$

$S_v \leq 1.71$ is a measure of the orderliness of a 2D set of points.⁷ On the other hand, disordered patterns built of asymmetric convex quadrangles with a zero VE were reported.⁸ Orderliness could not be exhaustively quantified with a single numerical parameter. Note also that VE and SE are different from Boltzmann thermodynamic entropy, as SE can be viewed as a kind of Shannon's measure of information.⁹

Note that VE does not depend on the number of points, which makes it an appropriate measure to compare the orderliness of structures with different numbers of points, such as molecules of different numbers of atoms.

Voronoi diagrams have been used to represent protein–ligand binding sites in proteins for machine learning applications;¹⁰ however, VE has not been used as a molecular descriptor to analyze ligands and their affinity to proteins. In this paper, we calculate the VE of 1144 potential drug-like molecules obtained from the BindingDB database as the COVID-19 data¹¹ to correlate it with the experimental values as half-maximal inhibitory concentrations (IC_{50}) determined from the SARS-CoV-2 main protease inhibition assays.

2. RESULTS AND DISCUSSION

2.1. Correlation between VE and Half-Maximal Inhibitory Concentration. The COVID-19 database ($n = 1144$) was used as a source for ligand molecules.¹² For each molecule, its SMILES (Simplified Molecular-Input Line-Entry System) description was used to create a molecular graph with atom coordinates using a standard Python chemoinformatic package RDKit.

VE was utilized as a molecular descriptor, S_v , to screen the database containing experimental IC_{50} values ($0.2 < IC_{50} < 1000$ nM). The analysis revealed a Gaussian distribution for the VE descriptor in the range $0.4 \leq S_v \leq 1.66$, with the most probable value of $S_v = 1.64$ (Figure 2a). The mean value of the number of atoms was 33.02 (Figure 2b).

To explore potential correlations between the IC_{50} and S_v parameters, the data set was divided into seven subsets with a step size of 0.2. Mean IC_{50} and S_v values were computed for each subset (Figure 3), and a linear regression model $IC_{50} =$

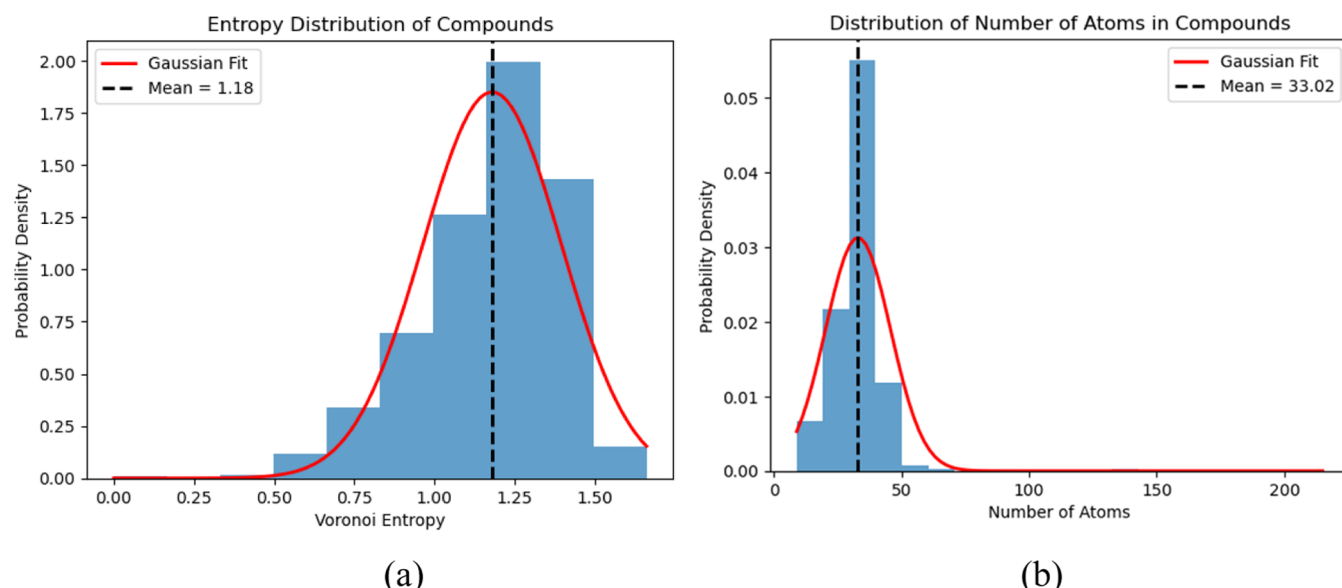


Figure 2. Frequency distribution of (a) VE and (b) the number of atoms for 1144 ligands.

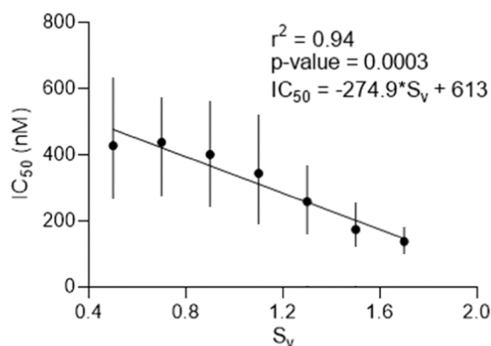


Figure 3. Correlation between the VE and affinity to the SARS-CoV-2 main protease (Mpro) represented by IC_{50} .

$-274.9 S_v + 613$ nM was established, showing a statistically significant correlation between the two parameters, with an r^2 value of 0.94 and a p-value of 0.0003 (p-value cutoff = 0.05).

2.2. Molecular Docking and Molecular Dynamics (MD) Simulations of Representative Molecules. Among the analyzed molecules, the two test compounds were chosen for molecular modeling due to their sharing of high and low entropy values. These values were computed for the sets of molecules ranking within the top 10 and bottom 10 in terms of IC_{50} .

The value $S_v = 1.41$ was found for the BDBM56411 ($C_{25}H_{29}F_3N_6O_4$), compound (1) molecule with $IC_{50} = 15$ nM, and the value $S_v = 0.78$ was found for the BDBM496040 molecule ($C_{20}H_{17}ClN_4O_2$), compound (2) with $IC_{50} = 667$ nM (Table 1 and Figure 4). Both molecules were tested to

Table 1. VE and Protein–Ligand Binding Affinities for Compounds 1 and 2 and the Reference Molecule

parameter	compound 1	compound 2	reference
S_v	1.41	0.78	1.22
IC_{50}	15	667	
ΔG_{bind}	-9.95	-9.36	-9.94
K_i	51.32	138.83	52.19
ΔG_{PBSA}	-6.97	0.76	-3.25
ΔG_{GBSA}	-39.97	-34.08	-46.44

inhibit the SARS-CoV-2 main protease (Mpro) using continuous fluorescence resonance energy transfer and the RapidFire MPro inhibition assays.¹³ A reference peptide-like molecule (N₃ inhibitor, or $C_{35}H_{48}N_6O_8$) was used to

determine the protein–ligand binding site within the Mpro structure.

To correlate protein–ligand interactions with IC_{50} and S_v values, rigid-flexible molecular docking was performed to calculate the affinity between compounds 1 and 2 and the Mpro protein (Figure 5a–d). The former ligand was found to bind the main protease with the highest affinity ($\Delta G_{bind} = -9.95$ kcal/mol).

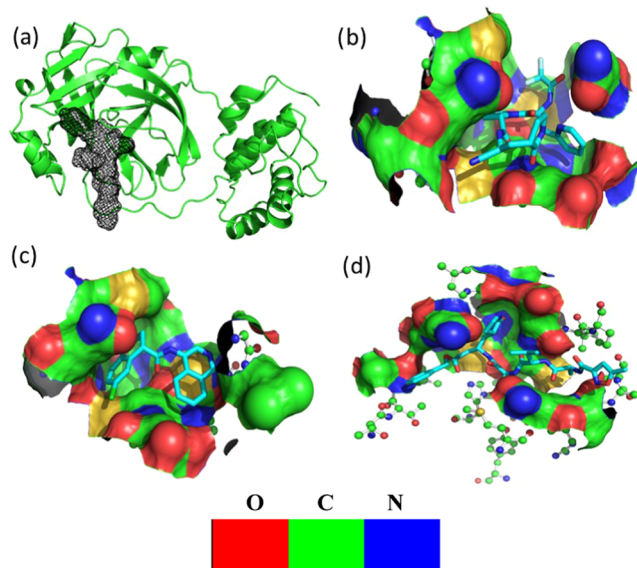


Figure 5. Docking of the compounds with the Mpro protein. Protein–ligand binding site is shown as black mesh (a). The binding conformations predicted from the AutoDock runs for compounds 1 (b) and 2 (c) and the N₃ inhibitor (d) bound to the Mpro structure were visualized. The molecular surface of the protein is used to highlight the binding site with colors representing the protein’s atomic composition. The protein residues are depicted as ball-and-stick models to clearly illustrate their positions. For the ligand molecules, a stick representation was employed, and hydrogen atoms were omitted to improve visual clarity.

To confirm the molecular docking results, the free energy of binding based on implicit solvation models (MM-PBSA/GBSA) was assessed for the analyzed protein–ligand complexes according to the standard protocol published elsewhere.^{14–17} These results confirmed the previous data, revealing much higher binding affinities for the comp1–Mpro

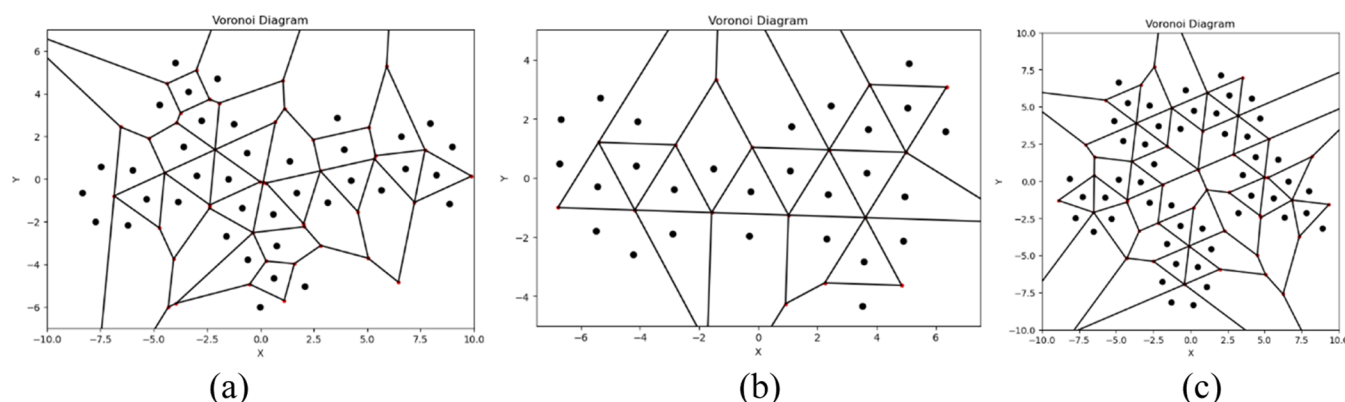


Figure 4. Voronoi diagrams of (a) compound 1, (b) compound 2, and (c) reference molecule.

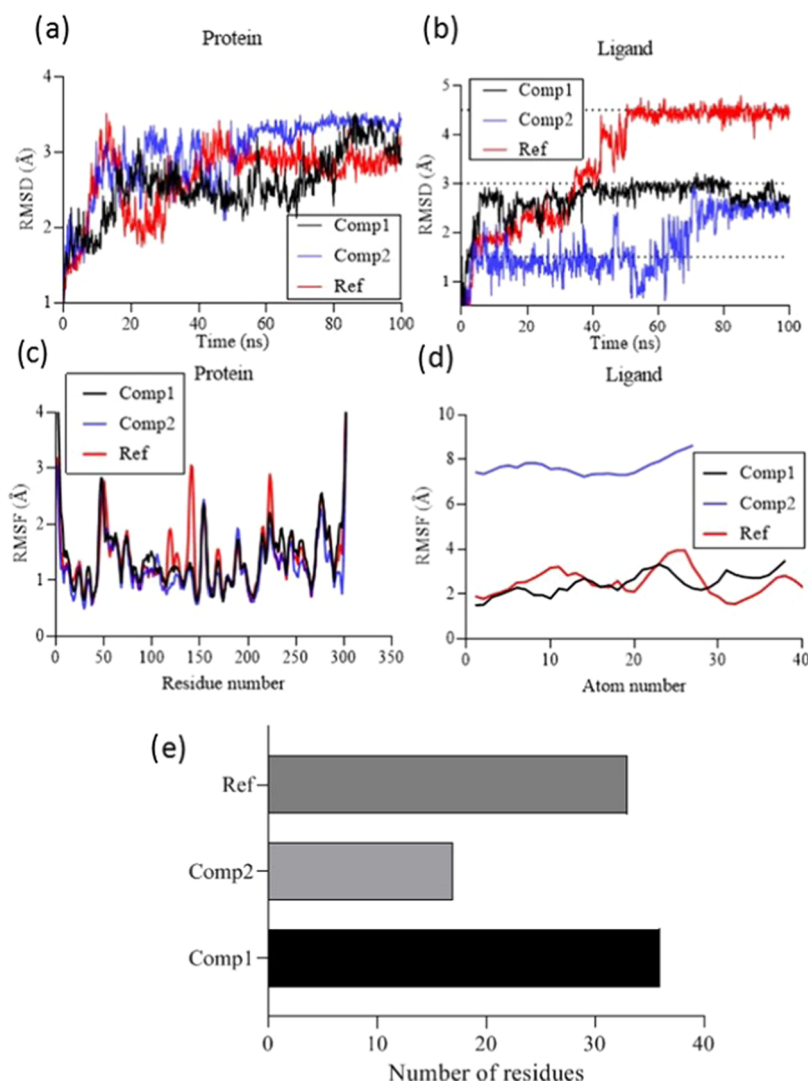


Figure 6. (a, b) RMSD (c, d), RMSF, and a number of residues involved in the (e) formation of H-bonds for comp1, comp2, and ref molecules bound to Mpro during 100 ns MD simulations.

complex (Table 1) in the PBSA model. Additionally, the MM-PBSA models indicated no binding for comp2–Mpro.

On the other hand, to explore the movements of the studied complexes, the root-mean-square deviation (RMSD) and fluctuation (RMSF) values, together with the number of residues involved in H-bonding, were plotted versus time (Figure 6). The protein RMSD values were in the range of about 3.0 Å for all complexes after the 80 ns time point (Figure 6a). The RMSD values for compounds 1 and 2 remained similar at the 3 Å threshold after 80 ns (Figure 6b), and the reference molecule experienced a much higher deviation of 4.5 Å, which stabilized after 50 ns. The protein RMSF values produced multiple peaks associated with highly flexible elements within the protein structures such as the N- and C-terminal parts, loops, turns, and random coils (Figure 6c).

The atomic fluctuations of compound 2 were at the 8.0 Å threshold (Figure 6d), probably indicating its high flexibility within the binding site. This can be explained by the fact that the ligand, being a relatively symmetric and ordered molecule ($S_v = 0.78$), is constrained in rotational motion, which decreases its chances of finding the optimal binding pose. Finally, the number of residues involved in H-bond formation between the protein and the ligand was evaluated for the

analyzed protein–ligand complexes. The highest number was determined for the comp1–Mpro complex, indicating its contribution to the highest protein–ligand affinity (Figure 6e).

2.3. Calculation of SE Based on SMILES. VE is a measure of the spatial orderliness and complexity of the molecules, which may determine their configurational space and correlate with their ability to bond to proteins. The question may be asked whether the information about the complexity is already contained in the molecular structure, for example, as presented by the SMILES description. While the Voronoi diagram is created from the original SMILES formula through several steps, the information characterizing molecular complexity may already be contained in the original formula.¹⁸ SE is the measure of redundancy of a text in any language, including molecular descriptions in the SMILES language. One can argue that the redundancy can be related to the constraints of the configuration space of a molecule and eventually to its ability to bind to proteins in RLIs.

To investigate the information content of the ligands, we studied the Shannon entropy of the SMILES formulas using

$$S_{\text{Sh}} = - \sum_n p_n \log_2 p_n$$

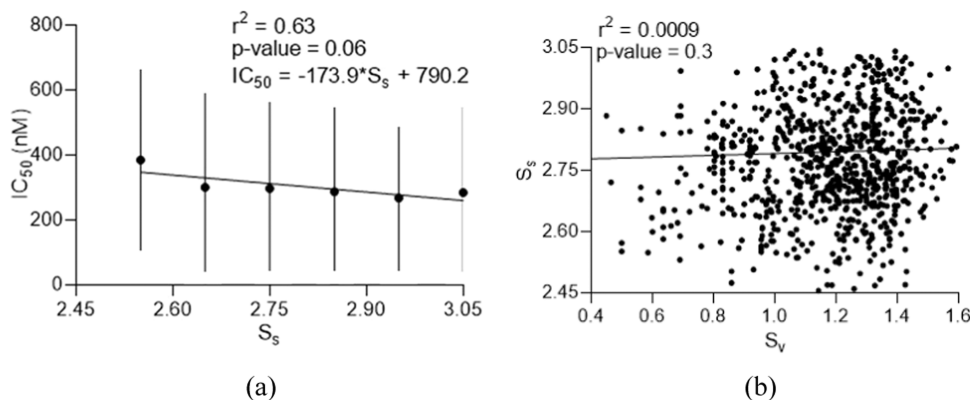


Figure 7. Correlation of (a) IC₅₀ and (b) VE with SE in the database of 1144 molecules.

where $0 \leq p_n \leq 1$ is the frequency of a “character” in the SMILES description (such as C, N, O, numbers, signs “−”, “=”, etc.). As a result, the SE molecular descriptor failed to provide enough evidence to reject the null hypothesis ($p\text{-value} > 0.05$) in the linear regression analysis with IC₅₀ values. (Figure 7a). Moreover, the correlation of VE and SE was studied as well, and no statistically significant correlation was observed (Figure 7b).

This suggests that the linear chain of characters in the SMILES language, while containing information about molecules, is insufficient to predict their binding properties in RLI.

3. DISCUSSION

Ligands are small molecules whose affinity for receptors is their crucial property. It was hypothesized that molecular mobility plays an important role in their ability to attach to receptors, and this mobility is related to asymmetry and less orderliness of the molecules. We suggested an algorithm that allows the use of VE as a molecular descriptor for predicting the affinity of ligands. First, the SMILES chemical formula is converted into a 2D graph. After that, the VE is calculated as a measure of the information content. The information about the molecule is also contained in the SMILES string. The information redundancy of SMILES was characterized by SE, but no statistically significant correlation was found. This strongly suggests that spatial arrangement is the key property controlling the affinity. The alphabet of the SMILES language consists of characters representing atomic elements, numbers, and bonds. On the other hand, the “alphabet” of the Voronoi diagram consists of polygons.

4. CONCLUSIONS

The Voronoi entropy molecular descriptor for 1144 ligands was calculated using a 2D projection. The Voronoi entropy was in the interval $0.4 \leq S_v \leq 1.66$, and its distribution was close to the Gaussian. The binding affinity of the ligands to the SARS-CoV-2 main protease was extracted from the COVID-19 database using the half-maximal inhibitory concentration (IC₅₀) data. A strong correlation with IC₅₀ was found, $IC_{50} = -274.9 S_v + 613$, indicating the important link between ligand complexity and affinity. On the other hand, no correlation of the SMILES-based SE molecular descriptor with IC₅₀ was found. These findings suggest that spatial 2D arrangements of ligand molecules rather than the redundancy

in their description affect their configurational space and, eventually, their ability to bind to receptors.

5. COMPUTATIONAL METHODS

The COVID-19 data ($n = 1144$) used in this study were obtained from the BindingDB database, which provides 2D molecules and corresponding IC₅₀ values in nM.⁷ The data were retrieved in the SDF file format, which contains the structural information on the molecules and their associated activity values. To analyze the data and derive meaningful insights, several computational tools were applied. Specifically, the RDKit package, a powerful and comprehensive cheminformatics library for Python, was utilized.¹⁹

The Python script was used to calculate the VE and SE of a set of 3D molecular structures represented as SMILES strings. The VE entropy, as a measure of molecular complexity, is calculated based on the Voronoi regions formed by the 3D coordinates of the atoms in each molecule. In a similar way, the SE of SMILES strings was calculated.

The scientific data analysis and visualization in this study were conducted using GraphPad Prism software.²⁰ The 3D coordinates of the COVID main protease (Mpro) (ID: 6LU7) in the complex with the N₃ inhibitor were retrieved from the PubChem database as a PDB file.²¹ Molecular docking was performed by using the AutoDock program with default settings. The protein–ligand binding site at Mpro was identified at the center of the cocrystallized reference molecules (N₃ inhibitor) using Cartesian coordinates $x = -10.8 \text{ \AA}$, $y = 12.61 \text{ \AA}$, and $z = 68.82 \text{ \AA}$. Grid maps were created using a grid spacing of 0.375 \AA with a dimension of 60 \AA . To prepare the structures for molecular docking, Gasteiger partial charges were assigned, and rotatable bonds were defined according to standard protocols.^{22,23} Docking output results were represented by the approximation function as the estimated Gibbs free energy of binding (ΔG_{bind}).

The molecular dynamics (MD) systems were solvated using the TIP3P water model and neutralized by adding Na⁺ ions using the tLEap input script from the AmberTools package. Long-range electrostatic interactions were modeled using the particle-mesh Ewald method.²⁴ The SHAKE algorithm²⁵ was used to constrain the length of covalent bonds involving hydrogen atoms. A Langevin thermostat was used to maintain the system temperature at 300 K. A time step of 2.0 fs was used for all of the MD simulations.

The minimization and equilibration phases were performed using 100,000 steps and a 1 ns period, respectively, in both

NVT and NPT ensembles. Subsequently, 100 ns classical MD simulations were performed for each protein–ligand complex in an NPT ensemble without constraints. The free energies (ΔG_{PBSA} and ΔG_{GBSA}) of the complexes were calculated using the Molecular Mechanics Poisson–Boltzmann or Generalized Born solvation models, augmented with a hydrophobic solvent-accessible surface area term (MM-PBSA and MM-GBSA),^{26,27} as a postprocessing end-state method.

■ ASSOCIATED CONTENT

Data Availability Statement

The data set is available at <https://github.com/virtualscreenlab/Voronoi>

■ AUTHOR INFORMATION

Corresponding Authors

Sergey Shityakov – Infochemistry Scientific Center (ISC), ITMO University, St. Petersburg 191002, Russia;
 orcid.org/0000-0002-6953-9771; Email: shityakoff@hotmail.com

Michael Nosonovsky – Infochemistry Scientific Center (ISC), ITMO University, St. Petersburg 191002, Russia; College of Engineering and Applied Science, University of Wisconsin-Milwaukee, Milwaukee, Wisconsin 53211, United States;
 orcid.org/0000-0003-0980-3670; Email: nosonovsky@infochemistry.ru.

Authors

Aleksandr S. Aglikov – Infochemistry Scientific Center (ISC), ITMO University, St. Petersburg 191002, Russia
Ekaterina V. Skorb – Infochemistry Scientific Center (ISC), ITMO University, St. Petersburg 191002, Russia;
 orcid.org/0000-0003-0888-1693

Complete contact information is available at:
<https://pubs.acs.org/10.1021/acsomega.3c07328>

Author Contributions

M.N. and S.S. conceived the study, performed theoretical analysis, and wrote most of the manuscript. S.S. and A.S.A. performed computational analysis and modeling and wrote corresponding sections of the manuscript. E.V.S. supervised and designed the study and helped to draft the manuscript. All authors gave final approval for publication.

Funding

This work was supported by the Ministry of Science and Higher Education of the Russian Federation, goszadanie FSER-2021-0013.

Notes

The authors declare no competing financial interest.
Ethics approval is not applicable, since the study did not include any human participants or animals. No fieldwork was involved in the study.

■ REFERENCES

- (1) Ballester, P. J.; Mitchell, J. B. O. A machine learning approach to predicting protein–ligand binding affinity with applications to molecular docking. *Bioinformatics* **2010**, *26* (9), 1169–1175.
- (2) Meng, Z.; Xia, K. Persistent spectral-based machine learning (PerSpect ML) for protein-ligand binding affinity prediction. *Sci. Adv.* **2021**, *7* (2021), No. eabc5329.
- (3) Cang, Z.; Wei, G.-W. Integration of element specific persistent homology and machine learning for protein-ligand binding affinity prediction. *Num. Methods Biomed. Eng.* **2018** *342*, e2914.
- (4) Zabrodsky, H.; Peleg, S.; Avnir, D. Continuous symmetry measures. *J. Am. Chem. Soc.* **1992**, *114*, 7843–7851.
- (5) Bormashenko, E.; Frenkel, M.; Legchenkova, I. Is the Voronoi Entropy a True Entropy? Comments on “Entropy, Shannon’s Measure of Information and Boltzmann’s H-Theorem”. *Entropy* **2017**, *19*, 48.
- (6) Frenkel, M.; Fedorets, A. A.; Dombrovsky, L. A.; Nosonovsky, M.; Legchenkova, I.; Bormashenko, E. Continuous Symmetry Measure vs Voronoi Entropy of Droplet Clusters. *J. Phys. Chem. C* **2021**, *125* (4), 2431–2436.
- (7) Bormashenko, E.; Frenkel, M.; Vilk, A.; Legchenkova, I.; Fedorets, A. A.; Aktaev, N. E.; Dombrovsky, L. A.; Nosonovsky, M. Characterization of Self-Assembled 2D Patterns with Voronoi Entropy. *Entropy* **2018**, *20*, 956.
- (8) Bormashenko, E.; Legchenkova, I.; Frenkel, M.; Shvalb, N.; Shoval, Sh. Voronoi Entropy vs. Continuous Measure of Symmetry of the Penrose Tiling: Part I. Analysis of the Voronoi Diagrams. *Symmetry* **2021**, *13* (9), 1659.
- (9) Ben-Naim, A. Entropy, Shannon’s Measure of Information and Boltzmann’s H-Theorem. *Entropy* **2017**, *19* (2), 48.
- (10) Feinstein, J.; Shi, W.; Ramanujam, J.; Brylinski, M. Bionoi: A Voronoi Diagram-Based Representation of Ligand-Binding Sites in Proteins for Machine Learning Applications. In *Protein-Ligand Interactions and Drug Design. Methods in Molecular Biology*; Ballante, F., Ed.; Humana: New York, NY, 2021; Vol. 2266 DOI: [10.1007/978-1-0716-1209-5_17](https://doi.org/10.1007/978-1-0716-1209-5_17).
- (11) Bonjack, M.; Avnir, D. The near-symmetry of protein oligomers: NMR-derived structures. *Sci. Rep.* **2020**, *10*, No. 8367.
- (12) Liu, T.; Lin, Y.; Wen, X.; et al. BindingDB: a web-accessible database of experimentally determined protein-ligand binding affinities. *Nucleic Acids Res.* **2007**, *35* (Database issue), D198–D201.
- (13) Boby, M. L.; et al. Open Science Discovery of Potent Non-Covalent SARS-CoV-2 Main Protease Inhibitors. *Science* **2023**, *382* (663), eabo7201.
- (14) Saleem, M.; Fareed, M. M.; Saani, M. S. A.; Shityakov, S. Network pharmacology and multitarget analysis of *Nigella sativa* in the management of diabetes and obesity: a computational study. *J. Biomol. Struct. Dyn.* **2023**, *1*–17.
- (15) Dutta, K.; Shityakov, S.; Maruyama, F. DSF inactivator RpFB homologous FadD upregulated in *Bradyrhizobium japonicum* under iron limiting conditions. *Sci. Rep.* **2023**, *13* (1), No. 8701.
- (16) Tamaian, R.; Porozov, Y.; Shityakov, S. Exhaustive in silico design and screening of novel antipsychotic compounds with improved pharmacodynamics and blood-brain barrier permeation properties. *J. Biomol. Struct. Dyn.* **2023**, *1*–22.
- (17) Shityakov, S.; Broscheit, J.; Förster, C. Alpha-Cyclodextrin dimer complexes of dopamine and levodopa derivatives to assess drug delivery to the central nervous system: ADME and molecular docking studies. *Int. J. Nanomedicine* **2012**, *7*, 3211–3219.
- (18) Guha, R.; Velegol, D. Harnessing Shannon entropy-based descriptors in machine learning models to enhance the prediction accuracy of molecular properties. *J. Cheminform.* **2023**, *15*, No. 54.
- (19) Bento, A. P.; Hersey, A.; Félix, E.; et al. An open source chemical structure curation pipeline using RDKit. *J. Cheminform.* **2020**, *12* (1), 51.
- (20) Mitteer, D. R.; Greer, B. D.; Fisher, W. W.; Cohrs, V. L. Teaching behavior technicians to create publication-quality, single-case design graphs in graphpad prism 7. *J. Appl. Behav. Anal.* **2018**, *51* (4), 998–1010.
- (21) Jin, Z.; Du, X.; Xu, Y.; et al. Structure of M(pro) from SARS-CoV-2 and discovery of its inhibitors. *Nature* **2020**, *582* (7811), 289–293.
- (22) Shityakov, S.; Förster, C. In silico predictive model to determine vector-mediated transport properties for the blood-brain barrier choline transporter. *Adv. Appl. Bioinform. Chem.* **2014**, *7*, 23–36.
- (23) Shityakov, S.; Skorb, E. V.; Förster, C. Y.; Dandekar, T. Scaffold Searching of FDA and EMA-Approved Drugs Identifies Lead

Candidates for Drug Repurposing in Alzheimer's Disease. *Front. Chem.* **2021**, *9*, 2021.

(24) Essmann, U.; Perera, L.; Berkowitz, M. L.; Darden, T.; Lee, H.; Pedersen, L. G. A smooth particle mesh Ewald method. *J. Chem. Phys.* **1995**, *103*, 8577–8593.

(25) Miyamoto, S.; Kollman, P. A. Settle: an analytical version of the SHAKE and RATTLE algorithm for rigid water models. *J. Comput. Chem.* **1992**, *13*, 952–962.

(26) Kollman, P. A.; Massova, I.; Reyes, C.; Kuhn, B.; Huo, S.; Chong, L.; et al. Calculating structures and free energies of complex molecules: combining molecular mechanics and continuum models. *Acc. Chem. Res.* **2000**, *33*, 889–897.

(27) Shityakov, S.; Roewer, N.; Förster, C.; Broscheit, J.-A. In silico investigation of propofol binding sites in human serum albumin using explicit and implicit solvation models. *Comput. Biol. Chem.* **2017**, *70*, 191–197.